CORPUS PUBLISHERS

Current Trends in Engineering Science (CTES)

ISSN: 2833-356X

Volume 3 Issue 4, 2023

Article Information

Received date : July 17, 2023

Published date: July 21, 2023

*Corresponding author

Alabodite Meipre George, Department of Maths/Computer Science, Nigeria

DOI: 10.54026/CTES/1036

Keywords

Cold water, Line plume, Buoyancy reversal, Numerical simulation

Distributed under Creative Commons CC-BY 4.0

Review Article

Flow Parameter Dependence of Laminar Plumes with Buoyancy Reversal from a Line Source

Alabodite Meipre George* and Evans Fiebibiseighe Osaisai

Department of Maths/Computer Science, Niger Delta University, Nigeria

Abstract

Laminar plumes that under goes buoyancy reversal have just been studied. It is true that fast penetration of the rising fluid will result to strong interaction between the rising plume and the ambient fluid which will lead to a quick halt based on the production of denser fluid that in turn halt their rise height. Thus, the present work have considered some sort of balance between viscous, inertia and buoyancy to have a reasonable plume's rise height and effective mixing as we observe the behavior of these rising plumes while varying Reynolds number. At initial time interval, plumes were symmetric. There was a sideways flapping and bobbing motion after when the penetrating head became dense and detached. Two regimes of Re dependence fountains height over the range of $Re \leq 200$ and the time τ_n taken to attain that height was recorded. Relations were also drawn that describes the rate of decrease in the fountain's height from our empirically determined data set. Profiles of temperature and the various velocity components were also determined. Thus, with the quadratic dependence relation assumption, laminar fountains are feasible for $Pr = 7$ or 11.4, $5 \leq Re \leq 200$ and 0.5 Fr. The fountains here are independent of Pr but dependent of both Re and Fr.

Introduction

Buoyancy driven flows are important and relevant in many practical applications based on the likelihood of buoyancy reversal especially in rising plumes in cold fresh water. This may be as a result of the nonlinear relation between temperature and density in water. This is feasible if we introduce a warm water discharge at the floor of any homogeneous and quiescent body of water or somewhere close to it, where the ambient dense fluid is considered to have a temperature below the temperature of maximum density (approximately 4°C) in fresh water. Once this is initiated, both fluid (warm water and ambient cold water) will in turn generate a more dense fluid through mixing which is also called cabling by Foster [1] as also recorded in [2,3]. In this, it is expected that an initially rising fluid because of its buoyancy will mix with the ambient fluid while penetrating further and in turn may form fountain as the most dense mixed fluid descend to the floor (Figure 1). Though, if the domain of configuration into consideration does not have greater depth, then the most buoyant fluid could rise to the lake surface and spread outwards forming surface gravity current. During this process, it is expected that the surface current will entrain cold water and stop spreading even as denser fluid descend to the floor [4]. Examples of such flow scenario can be found in Power station cooling water discharges. Such scenario can also be found in lakes, especially during the spring in a holomictic lake. Detailed explanation to this facts can be found in the literature review of [2-5].

It is very obvious that cooling water discharge from power stations will be turbulent but then, George et al. [2]; George & Kay [3] and Bukreev & Gusev [6] were able to experimentally and numerically considered plumes with buoyancy reversal at a low Reynold's number Re where the flow was laminar and in transition in some cases. Others have also considered laminar and turbulent plumes with buoyancy reversal though, with the assumption that density dependence on temperature is linear. With this assumption, it is expected that a negatively buoyant fluid is always injected upwards into a less dense ambient or the other way round. With this assumption, Lin, & Armfield, [7,8] have studied such plumes varying the flow parameters. Their findings showed that the fountain's height scaled $\frac{z_m}{x_0} = a_0 + a_1 Fr \mathrm{Re}^{-\frac{1}{2}} \frac{z_m}{x_0} = a_0 + a_1 Fr \mathrm{Re}^{-\frac{1}{2}}$ for $\mathrm{Re} \leq 200 \mathrm{Re} \leq 200$.

Where they also concluded that both fountains height and width are dependent on the flow parameters Froude number Fr and Reynold's number Re for axisymmetric and plane fountains. Williamson et al. [9] and Srinarayana et al. [10] have also considered laminar plane fountains experimentally over a range of low Reynolds number and Froude number. These authors could identify different regimes of flow behaviours which are either dependent or independent of the flow parameters. [11,12-16] can also provide us with more details into such flows. But then, it is worth noting that all these works as reviewed here considered fountains with the linear dependence relation assumption. Whereas, little attention has been given to plumes that undergoes buoyancy reversal as a result of the scenarios as indicated by [2,3,4,17]. Here, buoyancy reversal only need a nonlinear relation between density and the mixing ratio of both the warm and the ambient fluids. Thus, we assume density as a quadratic function of the mixing ratio, where the mixed fluid is less dense than the mean of the constituents densities [2-4]. More details can also be found in the literature of [2- 4,18].

Previously, George et al. [2] and George & Kay [3] have numerically considered laminar fountains with this assumption, fixing both Re, Pr and varied Froude number. In these studies, the behaviours as recorded were very similar to those with the linear relation assumption. But then, they were able to indicate a single regime of Fr dependence fountains height over the different ranges of Fr as compared to those by [10,12] where different regimes could be identified. The aim of this paper is to carryout another investigation on these fountains with the same quadratic assumption if there might be other possible behaviour and different regimes of flow varying Re over 5 Re 200. Both Froude and Prandtl numbers will be kept fixed at $Fr = 2.5$ and $Pr = 11.4$ respectively. Computational domain length and height will be kept constant, where length $L = 70x_{in}$, i.e., $0 \leq X \leq 70$, and a domain height $H = 56x_{in}$ i.e., $0 \leq Y \leq 56$ [2].

Copyright © George AM

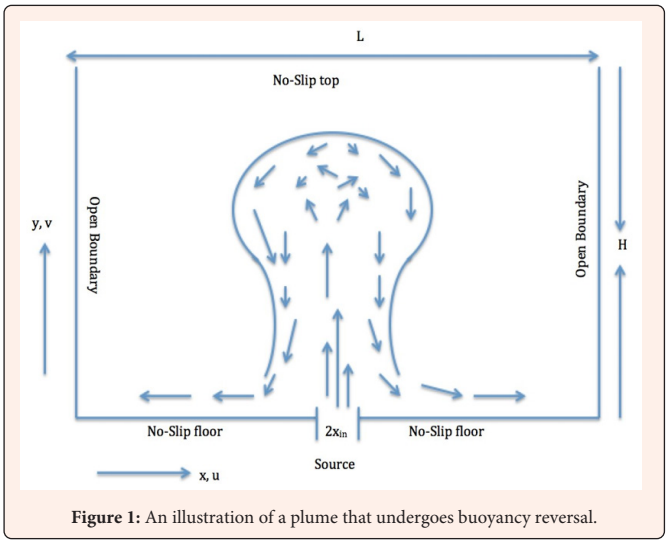

Figure 1: An illustration of a plume that undergoes buoyancy reversal.

Model Formulation and Governing Equations

Based on the nonlinear relation between density ρ and temperature T in water, we have considered the following relation suitable for this study,

$$\rho = \rho_m - \beta(T - T_m)^2 \quad (1)$$

It presents a better fit to the experimentally determined density of fresh water at temperature below 10°C taking T_m = 3.98 °C, $\rho_m = 1.000 \times 10^3$ kg.m^{-3} and $\beta = 8.0 \times 10^{-3}$ kg.m^{-3}(°C)$^{-2}$ [2,3,19,20] and other fluid properties such as viscosity, thermal diffusivity are assumed constant. We are proposing a two dimensional flow with time dependent study, where all the liquid properties are considered constant except for the water density, which changes with temperature and in turn results to the buoyancy force. We also assume a parabolic source velocity profile,

$$v(x,0) = \frac{3}{2} v_{in}\left[1 - \left(\frac{x}{in}\right)^2\right] \quad (2)$$

The input fluid temperature is T_{in} and this is assume to be constantly supplied at the centre of the domain of computation and a uniform initial ambient temperature T_∞. We assume that the dimensions for the domain of computation are not suitable length scales, as we consider them reliable for conditions at the sides and top to have no effect on the plume. Thus, we non-dimensionalise the coordinates x, y, velocity components u, v, time t, pressure p and temperature T by

$$U = \frac{u}{v_{in}} V = \frac{v}{v_{in}} X = \frac{x}{x_{in}} Y = \frac{y}{x_{in}} \tau = \frac{t}{x_{in}/v_{in}} P = \frac{p}{\rho v_{in}^2} \varphi = \frac{T - T_\infty}{T_m - T_\infty} \quad (3)$$

where x and u are horizontal, y and v are vertical [2].

We can also define our dimensionless parameters, the Reynolds Re, Prandtl Pr and Froude Fr numbers, by

$$\mathrm{Re} = \frac{v_{in} x_{in}}{\nu}, \quad \mathrm{Pr} = \frac{\nu}{\alpha}, \quad Fr^2 = \frac{\rho_m v_{in}^2}{g\beta(T_m - T_\infty)^2 x_{in}} \quad (4)$$

where ν and α are the respective diffusivities of momentum and heat, $\nu = \mu/\rho$ and $\alpha = k/\rho c_p$. Where, μ is viscosity, k is thermal conductivity and c_p is specific heat capacity. In terms of these dimensionless variables and parameters, the continuity equation, the horizontal and vertical momentum equations and the thermal energy equation are given as:

$$\frac{\partial U}{\partial X} + \frac{\partial V}{\partial Y} = 0 \quad (5)$$

$$\frac{\partial U}{\partial \tau} + U\frac{\partial U}{\partial X} + V\frac{\partial U}{\partial Y} = -\frac{\partial P}{\partial X} + \frac{1}{\mathrm{Re}}\left(\frac{\partial^2 U}{\partial X^2} + \frac{\partial^2 U}{\partial Y^2}\right) \quad (6)$$

$$\frac{\partial V}{\partial \tau} + U\frac{\partial V}{\partial X} + V\frac{\partial V}{\partial Y} = -\frac{\partial P}{\partial Y} + \frac{1}{\mathrm{Re}}\left(\frac{\partial^2 V}{\partial X^2} + \frac{\partial^2 V}{\partial Y^2}\right) \quad (7)$$

$$\frac{\partial \varphi}{\partial \tau} + U\frac{\partial \varphi}{\partial X} + V\frac{\partial \varphi}{\partial Y} = \frac{1}{\mathrm{RePr}}\left(\frac{\partial \varphi}{\partial X^2} + \frac{\partial \varphi}{\partial Y^2}\right) \quad (8)$$

Our initial conditions are an undisturbed, homogeneous medium as also given in [2].

$$U = 0, \quad V = 0, \quad \varphi = 0, \quad for \quad \tau < 0 \quad (9)$$

For $\tau \geq 0$ we have boundary conditions as follows. On the side walls:

$$\frac{\partial U}{\partial X} = 0, \quad \frac{\partial V}{\partial X} = 0, \quad \frac{\partial \varphi}{\partial X} = 0 \quad \text{at} \quad X = \pm\frac{L}{2x_{in}} \quad (10)$$

At the plume source:

$$U = 0, \quad V(X,0) = 1.5(1 - X^2), \quad \varphi = \varphi_{in} \quad for \quad |X| \leq 1 \quad at \quad Y = 0 \quad (11)$$

Elsewhere on the floor of the domain:

$$U = 0, \quad V = 0, \quad \frac{\partial \varphi}{\partial Y} = 0, \quad for \quad |X| > 1 \quad at \quad Y = 0 \quad (12)$$

At the top of the domain:

$$U = 0, \quad V = 0, \quad \frac{\partial \varphi}{\partial Y} = 0 \quad at \quad Y = \frac{H}{X_{in}} \quad (13)$$

The dimensionless temperature φ_{in} = 2.5 at the centre, and this is equal to a warm discharge at 10°C into an ambient temperature at 0°C. Method of solution is numerical by means of COMSOL Multiphysics software. We have used the "Extremely fine" settings for the mesh. Further information about the numerical methods is available from the COMSOL Multiphysics website [21]. We are going to show results by means of surface temperature plots of dimensionless temperature on a colour scale from dark red for the ambient temperature φ = 0.0, through yellow to white for the source temperature φ = 2.5. Note that φ = 1.0 also corresponds to the temperature of maximum density. Meanwhile, φ = 2 correspond to the temperature at which warm water has the same density as that of the ambient cold water [2-4].

Results

We have just simulated laminar plumes that undergoes buoyancy reversal and the progression of temper- ature field of these plumes are shown in figures 2- 8 for the various Reynolds numbers. Our previous results [3] have shown that very small Froude number Fr << 1 possesses greater buoyancy force and as such mixing could be vigorous irrespective of the Reynolds number within the range Re ≤ 100. Because the fast penetration of the rising fluid will result to strong interaction between the rising plume and the ambient fluid which will lead to a quick halt based on the production of denser fluid that in turn halt their rise height [3]. This implies that at Fr = 2.5, there is some kind of balance between inertia and buoyancy (reduced mixing as compared to Fr << 1). Meanwhile, for this range of Reynolds number (Re ≤ 100) it is true that viscous force will dominate, leading to a slow rise of the plume, and in the other way round reduced mixing. Thus, the present work have considered some sort of balance between viscous, inertia and buoyancy to have a reasonable plume's rise height and effective mixing as we observe the behaviour of these rising plumes while varying Reynolds number. As highlighted above, the results in figures 2 & 3 shows the time evolution of the plumes for Re = 5. The viscous force here is more dominant together with the reduced buoyancy force that have resulted in a very slow mixing enabling the plume to penetrate the ambient fluid farther. But then, as Re increases, it is evident that the viscous force decreases while inertia force is gradually becoming important (Figures 4-8) when comparing the various time of evolution in the figures. This implies that as Re increases keeping Fr fixed, the rising plumes collapse as a result of the mixed fluid that have attained Tm. From the various figures, it is clear that an initially rising plume which was symmetrical (Figure 2, 3(g), 4) experiences head detachment behaviour after the penetrating head became dense. This detached head in turn deflect the body of this rising plume sideways as it descend to the floor. Thereafter, this rising plume resulted into a flapping motion. There was also a bobbing motion whenever the descending dense fluid get cleared at the core of the rising plume. Meanwhile, the descended dense fluid that have attained the temperature of maximum density Tm or somewhere close to it will continue to spread outwards forming density current on the floor. Note that, the spreading behaviour of this density current is steady except for any perturbation by the arrival of new dense fluid from a detached head, which may cause oscillations downstream [2,3]. This is different from those by [23, 24] where the perturbation is as a result of the development of kelvin-Helmholtz instabilities at the interaction layer [2]. It is worth noting that all these behaviours as highlighted here have also been recorded in [2,3,9,10,12,22] thus, more insight and detailed explanation can be gained from them to avoid repetition.

We have earlier recorded that fountain's height increases with Froude number [2,3]. Whereas, the fountain's heights here in this present work appears different as Re increases, keeping both Froude and Prandtl number fixed. This is as a result of the increasing inertia force that enhances vigorous mixing which in turn lead to quick production of dense fluid that halt their rise height. This implies that fountain's height decreases with Reynolds number (Figure 9). In our introduction, we have indicated that previous results have shown three regimes of flow; though from those that have used the linear relation assumption [9,10, 12]. However [2,3] were able to identify a single regime of Fr dependence fountains height over the different ranges of Fr using the quadratic dependence assumption. Meanwhile, the present study could identify two regimes of Re dependence fountains height over the range of Re 200 and the time τ_n taken to attain that height and tabulated as shown in table 1, and plotted in Figures 9 & 10. This we have shown by the straight lines in (Figures 9 & 9d) and (10c & 10d) representing the best fit power laws obtained by linear regression of log Zn and log τ_n on log Re from our empirically determined data set: where R2 is the regression coefficient in each case. These regimes are evident in both the linear scale plot (Figures 9a & 10a) and that of the logarithmic scale plot (Figures 9a &10a).

$$Z_{n1st} = 40.123\,\mathrm{Re}^{-0.136} \qquad \left[R^2=0.7718\right] \qquad (14)$$

$$Z_{n2nd} = 36.663\,\mathrm{Re}^{-0.136} \qquad \left[R^2=0.9754\right], \qquad (15)$$

$$\tau_{n1st} = 205.73\,\mathrm{Re}^{-0.45} \qquad \left[R^2=0.997\right] \qquad (16)$$

$$\tau_{n2nd} = 96.727\,\mathrm{Re}^{-0.257} \qquad \left[R^2=0.9738\right] \qquad (17)$$

Our Re dependence scaling laws decreases with height in both regimes and as well as that of the time τ taken to reach the maximum rise height. It also showed that the rate of decrease in the fountain's height scaled the same in both regimes except for the constant of proportionality that scaled different. Whereas, the scaling laws for the time taken scaled differently in both regimes for the constant of proportionality and as well the rate of decrease. But then, the rate of decrease from the time taken suggest that difference in the time taken to attain maximum height for small Re (i.e., Re ≤ 30) is slightly much as compared to those for 40 ≤ Re ≤ 200. This resulted to the slightly sharp decline in the first regime for the time taken to attain maximum rise height.

We have also considered profiles of temperature and velocity components at the fountain's core (X = 0) in order to gain more insight (Figures 11-13). The temperature profiles are in agreement with the fact that fountains with smaller Re possesses greater viscous forces together with the moderately reduced buoyancy force from the Fr. This combination resulted in slow and very reduced mixing enabling the plume to penetrate the ambient fluid farther, before sufficiently significant dense fluid was produced to halt their rise height. Thus, it is evident that at the core of these fountains, significantly warm fluid could be noticed at a very reasonable height after a lengthy time of simulation. Whereas, mixing became a bit vigorous as Re increase. This is as a result of the increasing inertia force which enables quick penetration of the warm fluid (enhancing quick mixing as both fluid interact strongly) and in turn led to a quick production of dense fluid within a short time as compared to those of the smaller Re (Figures 11(a) - 11(c)). Though, the behaviour in the profiles of temperature appears similar to the cases for Fr dependent fountains height by George et al. [2] & George & Kay [3] fixing Re and varying Fr. In those results, smaller Fr possesses greater buoyancy force, enabling the plumes to penetrate faster and in turn resulted to the quick production of dense fluid that halts their rise height. From the profiles here it is also evident that decrease in temperature with height is not monotonic. Some of these fluctuations reaches their local maximum before decreasing sharply to the ambient temperature [2,3]. Furthermore, the velocity profiles at the fountain's core for the various components also agrees with the fact that there was a sideways flap- ping motion (Figure 13(a) -13(c)). Though, this is more evident in figure 13(c) which also confirm that as inertia force increases slightly vigorous mixing occurs somewhere very close to the fountain's source within the time range as considered here as compared to that in figure 13 (a) where viscous force is more dominant. Meanwhile, for the vertical velocity components we could observe some level of downward velocities within some time interval which indicates descending fluid. This downward or negative fluctuations are not common to all the figures but in figures 12(b) & 12(c) at much later time. This also confirm the fact that for fountain's with smaller Re could penetrate the ambient fluid farther before sufficiently dense or mixed fluid is produced that descends to the floor. This behaviour was also recorded in the cases for Fr dependent fountains by George et al. [2] & George & Kay [3].

Our primary aim in this study, is to see whether a different regime is guaranteed for a range of Reynolds numbers with the quadratic dependence relation assumption. Because, our previous results have showed just a single regime though, for Fr dependence fountain's height and those by Srinarayana et al. [10,12]. Though, the later was with the linear dependence relation assumption. Yes, two regimes were identified with the usual head detachment behaviour that is always distinct to fountains with the quadratic dependence assumption. Relations were also drawn that describes the rate of decrease in the fountain's height and shown in equation [14-17]. These relations are purely Re dependent unlike, those by [9-13] where Fountain's height is a function of both FrRe. But then, every other behaviours appears similar, except for the head detachment that is common to all those with the quadratic dependence assumption. Previous results have shown that the detached head for cases with higher Froude numbers could penetrate farther [2] which was not the case here. Thus, we can conclude that with the quadratic dependence relation assumption laminar fountains are feasible for Pr = 7 or 11.4, 5 ≤ Re ≤ 200 and 0.5 ≤ Fr. It is true that the power station cooling water discharge will be turbulent thus, investigation should be carried out so as to properly fathom the possible behaviours of turbulent fountains.

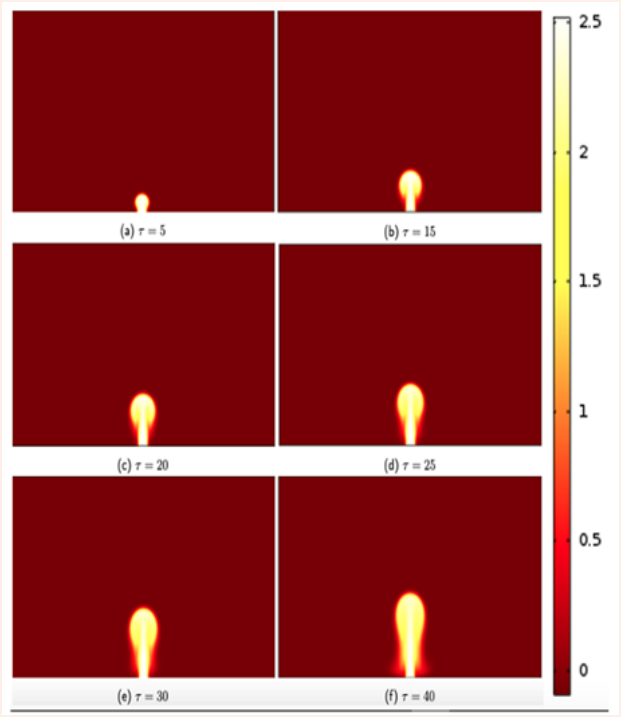

Figure 2: Progression of Temperature field for plumes with Re = 5, Pr = 11.4, φ_{in} = 2.5 and Fr = 2.5 at time 5 ≤ τ ≤ 40.

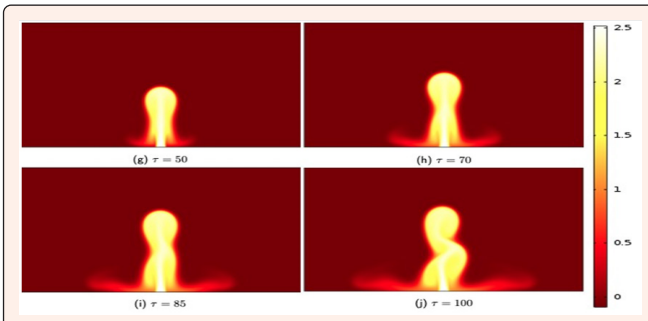

Figure 3: Progression of Temperature field for plumes with Re = 5, Pr = 11.4, φ_{in} = 2.5 and Fr = 2.5 at time 50 ≤ τ ≤ 100.

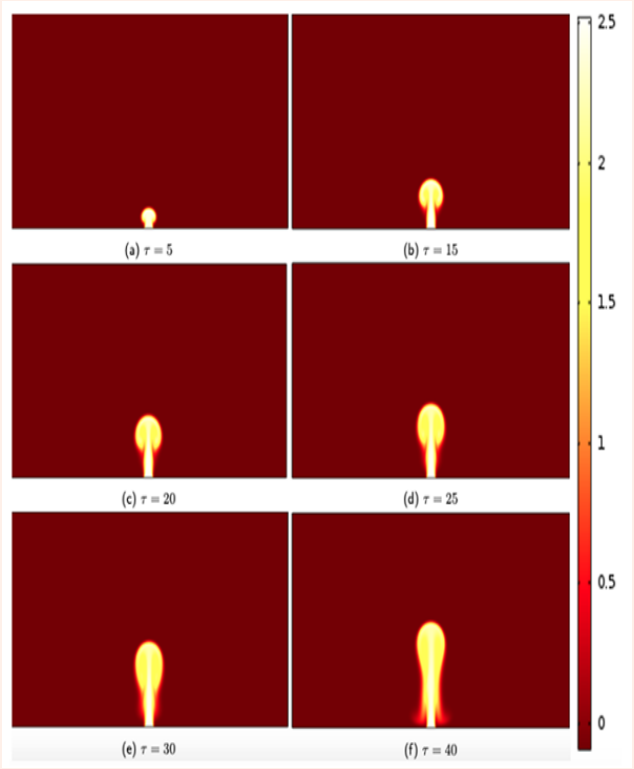

Figure 4: Progression of Temperature field for plumes with Re = 10, Pr = 11.4, φin = 2.5 and Fr = 2.5 at time $5 \leq \tau \leq 40$.

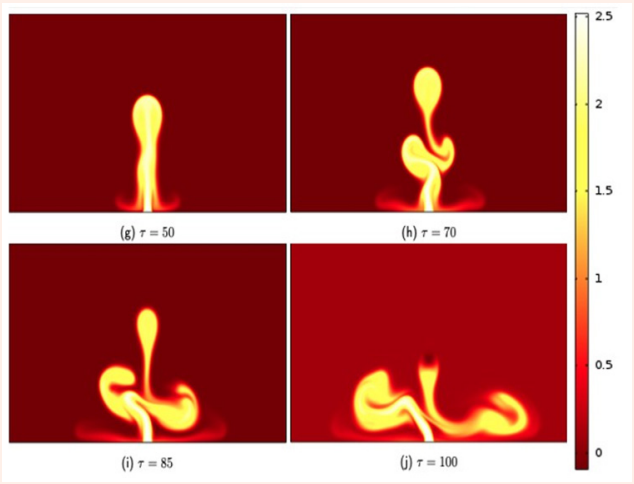

Figure 5: Progression of Temperature field for plumes with Re = 10, Pr = 11.4, φ_{in} = 2.5 and Fr = 2.5 at time $50 \leq \tau \leq 100$.

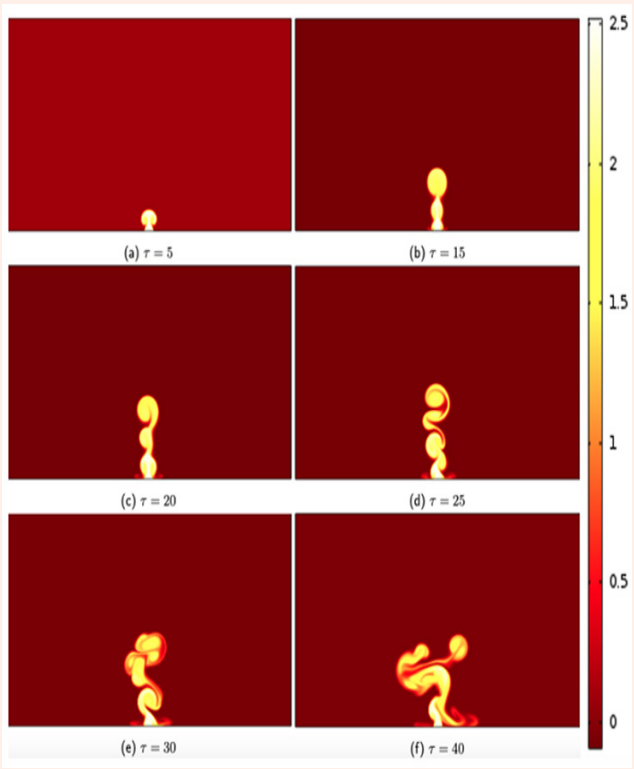

Figure 6: Progression of Temperature field for plumes with Re = 200, Pr = 11.4, φ_{in} = 2.5 and Fr = 2.5 at time $5 \leq \tau \leq 40$.

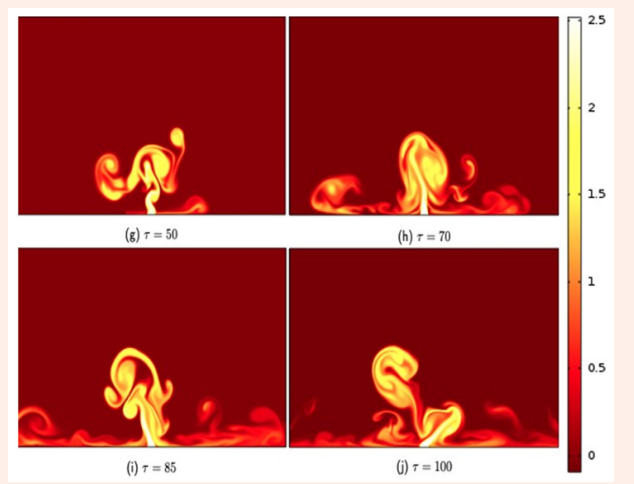

Figure 7: Progression of Temperature field for plumes with Re = 200, Pr = 11.4, φ_{in} = 2.5 and Fr = 2.5 at time $50 \leq \tau \leq 100$.

Copyright © George AM

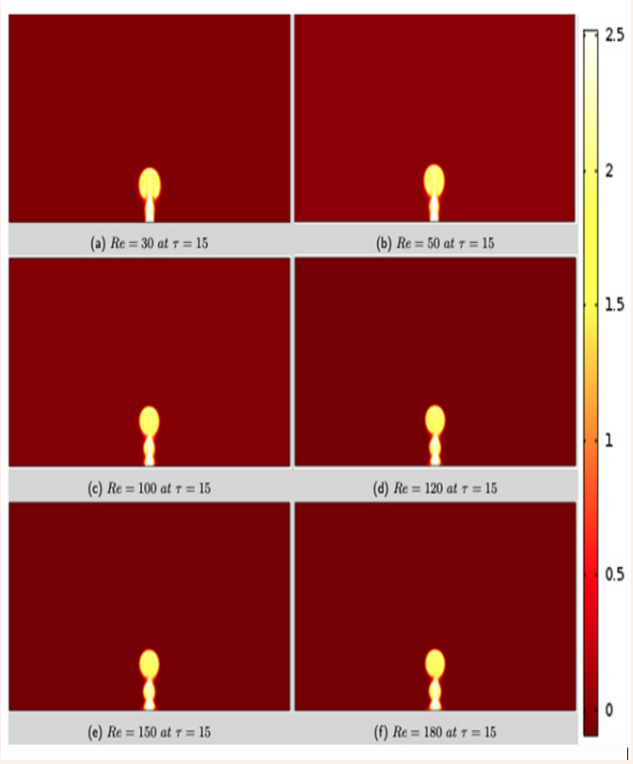

Figure 8: Progression of Temperature field for plumes with Re = 30, 50, 100, 120, 150, 180, Pr = 11.4, φ_{in} = 2.5 and Fr = 2.5 at time 15.

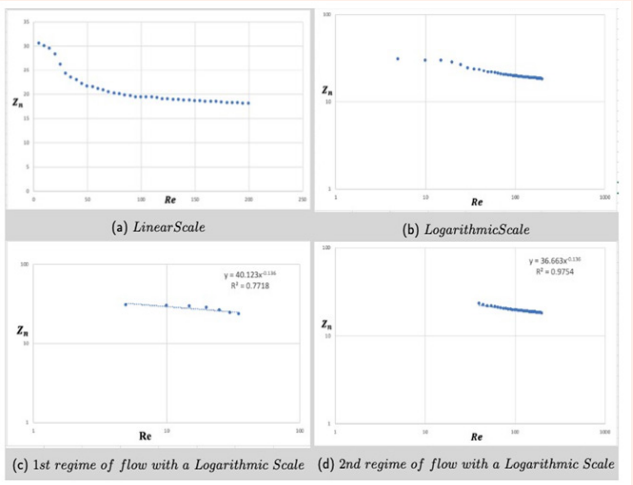

Figure 9: Change in the maximum plume's height with Reynold's number. Where panel (a) shows a linear scale plot, (b) a logarithmic scale, (c) first regime (d) second regime.

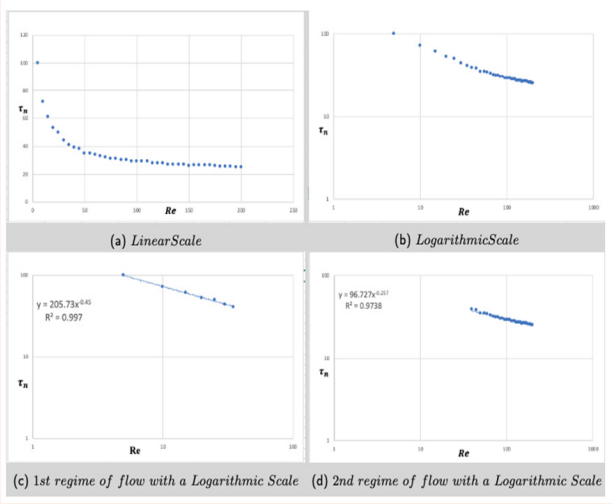

Figure 10: The time taken for plume to reach their maximum height with respect to Reynold's number. Where panel (a) shows a linear scale plot, (b) a logarithmic scale, (c) first regime (d) second regime.

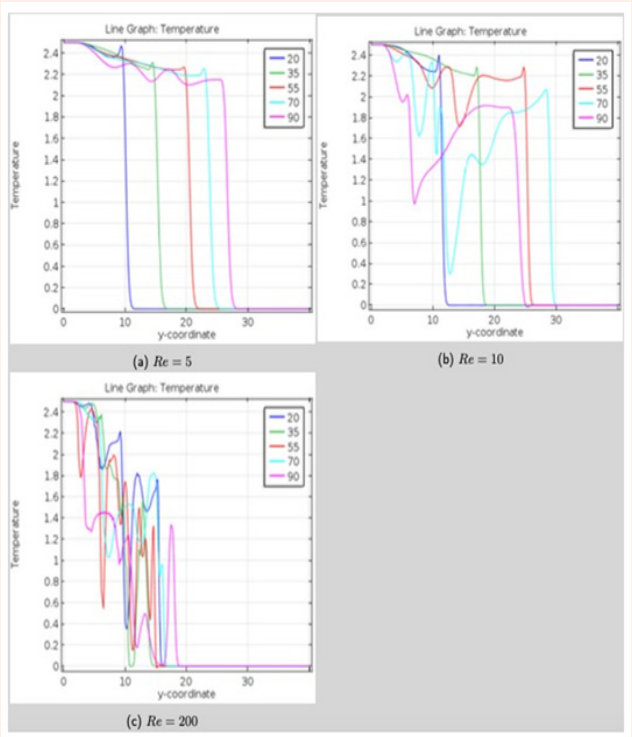

Figure 11: Dimensionless temperature distribution at the centreline $\varphi(0, y)$ for plumes with (a) Re = 5, (b) Re = 10, (c) Re = 200 at times τ = 20, 35, 55, 70, 90.

Copyright © George AM

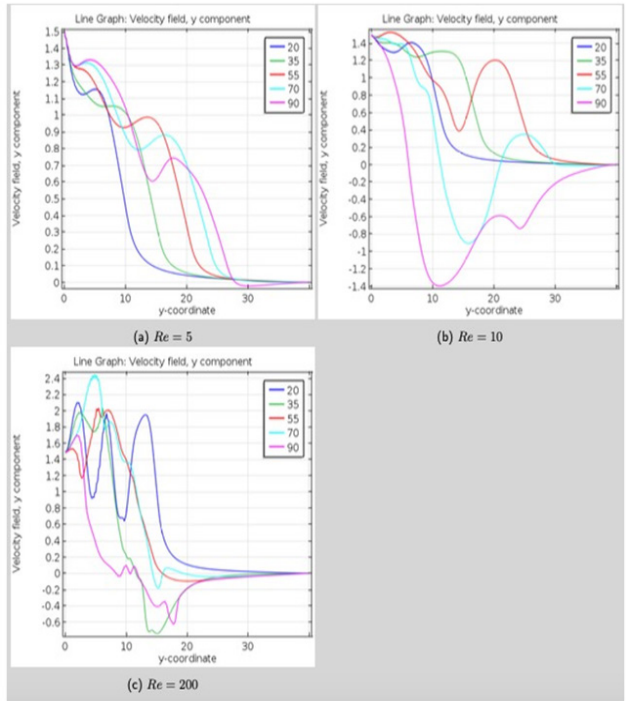

Figure 12: Dimensionless Y-component velocity distribution at the centreline V (0, y) for plumes with (a) Re = 5, (b) Re = 10, (c) Re = 200 at times τ = 20, 35, 55, 70, 90.

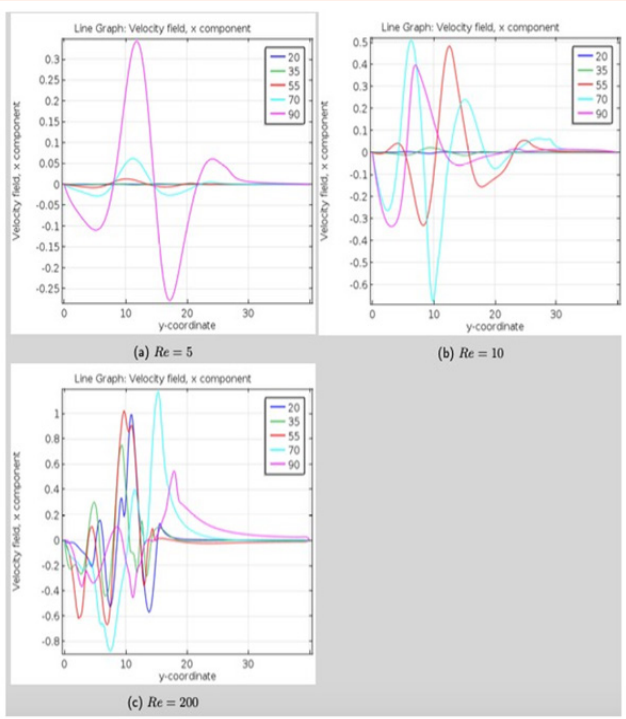

Figure 13: Dimensionless X-component velocity distribution at the centreline U (0, y) for plumes with (a) Re = 5, (b) Re = 10, (c) Re = 200 at times τ = 20, 35, 55, 70, 90.

Table 1: Maximum plume height Zn and time taken to reach that height at Froude numbers 5 ≤ Re ≤ 200.

Re	τ_n	Zn	Re	τ_n	Zn	Re	τ_n	Zn	Re	τ_n	Zn
5	100	30.52	55	35.0	21.471	105	29.0	19.35	155	26.6	18.512
10	72.0	29.953	60	34.0	21.117	110	29.0	19.311	160	26.6	18.498
15	61.0	29.538	65	33.0	20.779	115	28.0	19.234	165	26.6	18.415
20	53.0	28.311	70	32.0	20.444	120	28.0	19.03	170	26.6	18.4
25	50	26.201	75	31.0	20.193	125	28.0	18.98	175	26	18.347
30	44.0	24.243	80	31.0	20.016	130	27.0	18.819	180	25.6	18.234
35	41.0	23.469	85	30.0	19.77	135	27.0	18.81	185	25.6	18.213
40	39.0	22.92	90	30.0	19.671	140	27.0	18.739	190	25.6	18.191
45	38.0	22.158	95	29.0	19.4	145	27.0	18.658	195	25	18.095
50	35.0	21.66	100	29	19.38	150	26.0	18.522	200	25	18.062

Summary/Conclusion

Laminar plumes that under goes buoyancy reversal have just been studied using the assumption that density was taken as a quadratic function of temperature. It is true that fast penetration of the rising fluid will result to strong interaction between the rising plume and the ambient fluid which will lead to a quick halt based on the production of denser fluid that in turn halt their rise height. Thus, at Fr = 2.5 there is some kind of balance between inertia and buoyancy (reduced mixing as compared to Fr << 1) because smaller Froude numbers possesses greater buoyancy force. Meanwhile, for this range of Reynolds number (Re 100) it is true that viscous force will dominate leading to a slow rise of the plume, and in the other way round reduced mixing. Thus, the present work have considered some sort of balance between viscous, inertia and buoyancy to have a reasonable plume's rise height and effective mixing as we observe the behaviour of these rising plumes while varying Reynolds number. At initial time interval, plumes were symmetric. This symmetric behaviour was maintained for a longer time for plumes with smaller Re before sufficiently buoyant fluid was produced to halt their height. There was a sideways flapping and bobbing motion after when the penetrating head became dense and detached. We could identify two regimes of Re dependence fountains height over the range of Re 200 and the time τ_n taken to attain that height. Relations were also drawn that describes the rate of decrease in the fountain's height from our empirically determined data set. Most of the behaviours as observed here are also similar to those by previous authors as indicated above. Profiles of temperature and the various velocity components were also determined to gain insight of such flows and they agree with the various behaviours as described above. Thus, we can conclude that with the quadratic dependence relation assumption laminar fountains are feasible for Pr = 7 or 11.4, 5 Re 200 and 0.5 ≤ Fr. It is true that the power station cooling water discharge will be turbulent thus, investigation should be carried out so as to properly fathom the possible behaviours of turbulent fountains.

References

1. Foster TD (1972) An analysis of the cabbeling instability in sea water. Journal of Physical Oceanography 2(3): 294-301.
2. George MA, Osaisai FE, Dienagha N (2023) Laminar Plumes from a Line Source and Their Possible Flow Behaviours. Asian Research Journal of Mathematics 19(4): 15-30.
3. George MA, Kay A (2017) Warm discharges in cold fresh water: 2. Numerical simulation of laminar line plumes Environ. Fluid Mech 17: 231-246.
4. George MA, Kay A (2017) Numerical simulation of a line plume impinging on a ceiling in cold fresh water. International Journal of Heat and Mass Transfer 108: 1364-1373.
5. Hoglund B, Spigarelli SA (1972) Studies of the sinking plume phenomenon. In: Proceedings of the 15th conference on great lakes research. International Association of Great Lakes Research, Ann Arbor, pp. 614-624.

6. Bukreev VI, Gusev AV (2011) The effect of densification during mixing on the spreading of a vertical round jet Doklady. Earth Sciences 439(1): 1002-1005.

7. Lin W, Armfield WS (2000) Direct simulation of weak laminar plane fountains in a homogeneous fluid. International Journal of Heat and Mass Transfer 43: 3013-3026.

8. Lin W, Armfield WS (2000) Direct simulation of weak axisymmetric fountains in a homoge- neous fluid. Journal of Fluid Mechanics 403: 67-88.

9. Williamson N, Srinarayana N, Armfield WS, McBain DG, Lin W (2008) Low-Reynolds- number fountain behaviour. Journal of Fluid Mech 608: 297-317.

10. Srinarayana N, Williamson N, Armfield WS, Lin W (2010) Line fountain behaviour at low Reynolds number. International Journal of Heat and Mass Transfer 53(9-10): 2065-2073.

11. Lin W, Armfield WS (2003) The Reynolds and Prandtl number dependence of weak fountains. Comput Mech 31: 379-389.

12. Srinarayana N, McBain DG, Armfield WS, Lin W (2008) Height and stability of laminar plane fountains in a homogeneous fluid. International Journal of Heat and Mass Transfer 51(19-20): 4717-4727.

13. Srinarayana N, Armfield WS, Lin W (2013) Behaviour of laminar plane fountains with a parabolic inlet velocity profile in a homogeneous fluid. International Journal of Therm Sci 67: 87-95.

14. Hassanzadeh H, Eslami A, Taghavi SM (2021) Positively buoyant jets: Semi-turbulent to fully turbulent regimes. Journal of Physical Review Fluids 6(5): 1-32.

15. Xue N, Khodaparast S, Stone HA (2019) Fountain mixing in a filling box at low Reynolds numbers. Journal of Physical Review Fluids 4(2): 1-13.

16. Dong L, Lin W, Armfield WS, Kirkpatrick PM, Williamson N, et al. (2022) Direct numerical simulation of fountain filling box flow with a confined weak laminar plane fountain. Journal of Heat Transfer 52(1): 193-215.

17. Marmoush YR, Smith AA, Hamblin PF (1984) Pilot experiments on thermal bar in lock exchange flow. Journal of Energy Engineering - ASCE 110: 215-227.

18. Kay A (2007) Warm discharges in cold fresh water: 1. Line plumes in a uniform ambient. Journal of Fluid Mech 574: 239-271.

19. Moore DR (1973) Nonlinear penetrative convection. Journal of Fluid Mech 61(3): 553-581.

20. Oosthuizen PH (1996) A numerical study of the steady state freezing of water in an open rectan- gular cavity. Int J Numer Meth Heat Fluid Flow 6: 3-16.

21. (2016) COMSOL Multiphysics Cyclopedia. The Finite Element Method (FEM).

22. Vinoth BR, Panigrahi PK (2014) Characteristics of low Reynolds number non-Boussinesq fountains from non-circular sources. Phys Fluids 26: 014106.

23. George MA, Osaisai FE (2022) A Numerical Study of the behaviour on Lock Volume Variations in Lock-Exchange Density Current in Cold Fresh Water. Journal of Scientific Research & Reports 28(10): 125-141.

24. George MA, Osaisai FE (2022) Density Current Simulations In Cold Fresh Water And Its Cabbeling phenomenon: A Comparative Analysis With Given Experimental Results Current. Journal of Applied Science and Technology 41(29): 37-52.